ISSN 2616-5775 Vol. 9, Issue 7: 34-43, DOI: 10.25236/AJCIS.2026.090705

Behavior-Driven SOC and Time-to-Empty Prediction for Smartphone Batteries Using a Continuous-Time Electro-Thermal Model

Bo Yan[1,a,*], Kaiyuan Yang[1,b], Junyan Yang[1,c]

[1]*College of Science and Technology, Beijing Normal University-Hong Kong Baptist University United International College, Zhuhai, China*
[a]*yanbo18647112800@163.com*, [b]*1765777605@qq.com*, [c]*1285783343@qq.com*
**Corresponding author*

Abstract: *Accurate smartphone time-to-empty (TTE) prediction requires a model that links user behavior, device-level power demand, and battery electro-thermal dynamics. This paper presents a continuous-time framework for predicting state of charge (SOC) and TTE under behavior-driven operating conditions. Screen brightness, CPU utilization, network activity, and background workload are represented as time-varying behavioral inputs and mapped to demand power through an interpretable additive formulation. The resulting power demand is constrained by achievable device power and coupled with a battery power-closure equation, where terminal voltage is described by an OCV-SOC relationship with temperature-dependent internal resistance. A lumped thermal balance is used to model Joule heating and heat dissipation, and the temperature state feeds back to effective capacity, internal resistance, and efficiency. The coupled differential-algebraic system is solved through fixed-step time marching to obtain SOC, voltage, temperature, and TTE trajectories. An OAT sensitivity analysis indicates that TTE is dominated by the capacity/energy scale and load-side behavior-to-power mapping, with importance values of 59.30% and 37.72%, respectively. Thermal and environmental effects account for 2.99% under the selected TTE metric, while resistance and efficiency terms exhibit weak first-order identifiability. The results suggest that reliable endurance prediction and optimization should prioritize usable-capacity estimation and load-side power reduction, with thermal control retained as a secondary but necessary mechanism for high-load robustness.*

Keywords: *smartphone battery; state of charge; time-to-empty; electro-thermal coupling; behavior-driven power; sensitivity analysis*

1. Introduction

Smartphone battery endurance has become a critical constraint on mobile computing because the user-perceived remaining time is determined by both software behavior and battery physical response. Large-scale Android battery datasets show that charge and discharge behavior varies with device model, system setting, application context, and network condition [1]. User-level power modeling studies further indicate that brightness, data activity, radio state, and other usage-dependent variables can be used to predict smartphone power consumption [2]. At the hardware level, modern mobile application processors introduce additional complexity because multicore CPUs, GPUs, multimedia engines, GPS, Wi-Fi, and cellular interfaces contribute to time-varying power demand [3]. Recent reviews of mobile software energy estimation also show that energy profiling remains difficult because application behavior, operating-system services, and hardware states interact across multiple layers [4].

Battery-side modeling provides the physical basis for converting device power demand into SOC and TTE trajectories. The general battery energy-balance formulation establishes heat generation and dissipation as necessary components of physically meaningful battery models [5]. Equivalent-circuit models have been widely adopted because they offer a tractable representation of OCV, internal resistance, and transient voltage response while remaining suitable for online computation [6]. Broader surveys of equivalent-circuit and electrochemical models also show that reduced-order models are often preferred when real-time simulation and control are required [7]. For SOC determination, OCV-based calibration, ampere-hour integration, regression, and model-assisted estimation have been extensively discussed, but their accuracy depends strongly on model structure, current measurement, temperature, and battery aging [8]. Kalman-filter-based methods provide a rigorous framework for state

ISSN 2616-5775 Vol. 9, Issue 7: 34-43, DOI: 10.25236/AJCIS.2026.090705

and parameter estimation in battery management systems [9], and SOC management reviews emphasize that reliable estimation must jointly consider model uncertainty, measurement noise, operating condition, and calibration strategy [10].

Temperature further complicates TTE prediction because it affects internal resistance, available capacity, efficiency, and voltage deliverability. Lumped thermal models have been shown to capture the dominant thermal behavior of cylindrical lithium-ion cells with acceptable computational cost [11]. Electro-thermal battery models further demonstrate that electrical states, heat generation, surface temperature, and core temperature should be coupled when predicting battery behavior under dynamic loads [12]. These studies support the use of a compact electro-thermal formulation in smartphone TTE prediction, where the model must remain simple enough for engineering interpretation but rich enough to represent feedback from current to temperature and from temperature to SOC depletion.

Long-term degradation is also relevant because capacity fade and resistance growth change the same parameters that determine short-term endurance. Reviews of lithium-ion aging mechanisms show that capacity loss and impedance increase are driven by multiple electrochemical and operating-condition-dependent processes [13]. State-of-health estimation studies further indicate that practical SOH evaluation remains challenging because degradation indicators depend on usage history, temperature, load profile, and measurement availability [14]. Electrochemical impedance spectroscopy has been widely used to characterize aging phenomena and relate impedance components to degradation mechanisms, but such analysis usually requires a separate life-cycle modeling framework [15]. Therefore, in the present paper, aging is treated as an extension through slow-varying capacity and resistance parameters rather than as an independent core model.

Based on the above literature, the main gap is that smartphone power modeling and battery electro-thermal modeling are often developed separately. A model that predicts TTE for smartphones should connect user behavior to demand power, map achievable power to current through voltage closure, update temperature through heat balance, and integrate SOC through charge conservation. This study therefore addresses two research questions: how to construct a continuous-time electro-thermal SOC-TTE model for smartphones, and which factors dominate TTE variation under representative operating conditions.

The contribution of this paper is threefold. First, it formulates an interpretable behavior-driven power demand model using screen, CPU, network, and background workload inputs. Second, it couples this demand model with a continuous-time electro-thermal SOC model based on OCV-SOC voltage, internal resistance, power closure, heat balance, and temperature-corrected effective capacity. Third, it uses sensitivity analysis to identify the dominant sources of TTE variation and to derive engineering implications for capacity estimation, load reduction, and thermal management.

2. Continuous-time electro-thermal SOC model

The proposed model describes the discharge process of a smartphone battery in continuous time. The primary state variables are the SOC $S(t)$ and battery temperature $T(t)$. The external inputs are screen brightness $u_s(t)$, CPU load $u_c(t)$, network activity $u_n(t)$, background activity $u_b(t)$, and environmental temperature $T_{env}(t)$. The model outputs include SOC(t), terminal voltage $V(t)$, temperature $T(t)$, discharge current $I(t)$, and the predicted TTE.

2.1 Behavior-Driven Power Demand

At the device level, power demand is represented as the superposition of baseline power and the contributions of major behavior-related modules. The additive structure is selected because it is physically interpretable, parsimonious, and directly suitable for sensitivity analysis:

$$P_{dem}\left(t\right)=P_0+a_s u_s\left(t\right)+a_c u_c\left(t\right)+a_n u_n\left(t\right)+a_b u_b\left(t\right) \tag{1}$$

where P_0 denotes standby power, and a_s, a_c, a_n, and a_b are coefficients that map screen, CPU, network, and background activity levels to their corresponding power contributions. Because practical smartphones impose power limits through operating-system control, thermal throttling, and battery protection, the demand power is converted into achievable power as follows:

ISSN 2616-5775 Vol. 9, Issue 7: 34-43, DOI: 10.25236/AJCIS.2026.090705

$$P_{act}(t) = \mathrm{soft}_{\mathrm{clip}}(P_{dem}(t), P_{max}(S,T)) \tag{2}$$

where $P_{max}(S,T)$ denotes the maximum deliverable or permitted power under the current SOC and temperature. This constraint improves numerical stability and reflects the fact that not all requested power points are physically or operationally feasible.

2.2 Electrical Power Closure

The electrical layer determines the discharge current corresponding to the achievable power. The terminal voltage is modeled using an OCV-SOC relation and an ohmic internal-resistance drop:

$$V(t) = OCV(S) - I(t)R(T) \tag{3}$$

The actual power delivered by the battery satisfies the power-closure relation:

$$P_{act}(t) = V(t)I(t) \tag{4}$$

Substituting Eq. (3) into Eq. (4) yields a quadratic equation for the discharge current:

$$RI^2 - OCV \cdot I + P_{act} = 0 \tag{5}$$

The corresponding instantaneous current is given by:

$$I(t) = \frac{OCV(S) \pm \sqrt{OCV(S)^2 - 4R(T)P_{act}(t)}}{2R(T)} \tag{6}$$

The discriminant Delta= $\sqrt{OCV(S)^2 - 4R(T)P_{act}(t)}$ provides a feasibility condition for the operating point. A negative discriminant indicates that the requested power cannot be delivered under the current voltage and resistance state, and therefore requires power limiting or is treated as an infeasible state. Under normal discharge, the physically admissible current root is selected for time integration.

2.3 Thermal Coupling

Internal resistance is assumed to vary with temperature according to a first-order approximation:

$$R(T) = R_0\left[1 + k_T(T - T_{ref})\right] \tag{7}$$

Battery temperature is then described by a lumped heat-balance equation that includes Joule heat generation and heat dissipation to the environment:

$$mC_p\frac{dT}{dt} = I^2R(T) - hA(T - T_{env}) \tag{8}$$

where $_mC_p$ is the equivalent heat capacity and hA is the equivalent heat-transfer coefficient. This formulation captures the main electro-thermal feedback pathway: current produces heat through internal resistance, temperature changes the resistance and effective capacity, and these changes subsequently influence current and SOC depletion.

2.4 SOC Dynamics

SOC evolution is derived from charge conservation. Temperature-dependent capacity and efficiency corrections are included to account for performance variation away from the reference temperature:

$$\frac{dS}{dt} = -\frac{I(t)}{Q_{eff}(T)}\eta(T) \tag{9}$$

ISSN 2616-5775 Vol. 9, Issue 7: 34-43, DOI: 10.25236/AJCIS.2026.090705

The temperature-correction terms are expressed as:

$$Q_{eff}(T) = Q_{eff}\left[1 - k_Q \,|\, T - T_{ref} \,|\right], \quad \eta(T) = 1 - k_\eta \,|\, T - T_{ref} \,| \tag{10}$$

Equations (1)-(10) define a closed behavior-power-electro-thermal-SOC system:

$$u(t), T_{env} \Rightarrow P_{dem} \Rightarrow P_{act} \Rightarrow I, V \Rightarrow T, S \Rightarrow R(T), Q_{eff}(T), \eta(T), OCV(S) \tag{11}$$

This structure preserves the causal sequence from user behavior to power demand and from battery response to TTE. It also keeps the model sufficiently compact for engineering interpretation and parameter-sensitivity analysis.

2.5 Numerical Solution and TTE Definition

The complete model is a differential-algebraic system. At each time step t_k, the algorithm evaluates $P_{dem}(S,T)$, applies the power constraint to obtain $P_{act}(t_k)$, solves the current from the quadratic power-closure equation, and updates temperature and SOC using fixed-step integration:

$$T_{k+1} = T_k + \Delta t \frac{I_k^2 R_k - hA(T_k - T_{env,k})}{mC_p} \tag{12}$$

$$S_{k+1} = S_k + \Delta t \left[-\frac{I_k}{Q_{eff}(T_k) \cdot 3600} \right] \eta(T_k) \tag{13}$$

The simulation terminates when SOC reaches the depletion threshold, terminal voltage falls below the cut-off voltage, or the current solution becomes infeasible. TTE is defined as the first time at which the depletion threshold is reached. The same time-marching procedure outputs the complete SOC, voltage, and temperature trajectories for a specified usage profile.

3. Experimental Results

Public battery and usage data are used to parameterize and illustrate the proposed framework. CALCE OCV and dynamic-load data support construction of the OCV-SOC curve and internal-resistance fitting. Smartphone usage records, such as those from the GreenHub dataset, or scenario-defined behavior sequences can provide the external inputs for screen, CPU, network, and background activity. Figure 1 summarizes the resulting SOC-TTE prediction workflow.

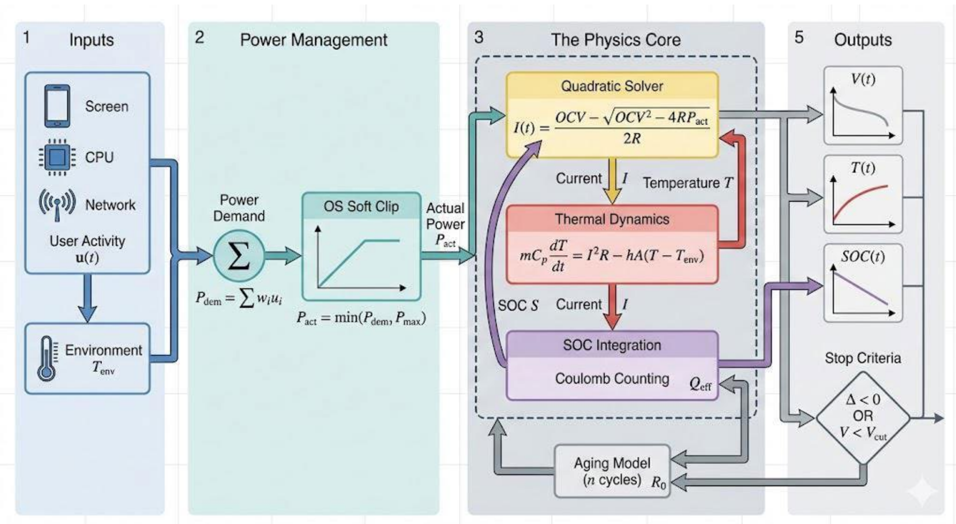

Figure 1. Framework of the proposed SOC-TTE prediction model.

The OCV-SOC curve in Figure 2 provides the OCV(S) input for the terminal-voltage equation. The

ISSN 2616-5775 Vol. 9, Issue 7: 34-43, DOI: 10.25236/AJCIS.2026.090705

fitted curve exhibits a clear nonlinear relationship between SOC and open-circuit voltage, with relatively flat plateau regions appearing at high and low SOC ranges and an approximately linear variation in the mid-SOC interval. This behavior is consistent with the electrochemical characteristics of lithium-ion batteries and ensures that the voltage model can realistically capture the variation of terminal voltage during the discharge process. The close agreement between measured OCV samples and the fitted curve further indicates that the interpolation-based representation is sufficiently accurate for continuous-time simulation.

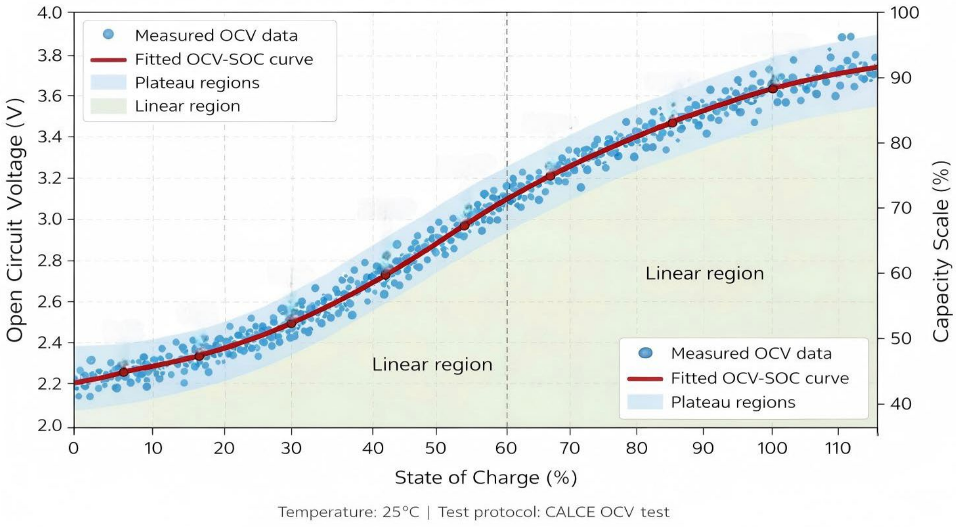

Figure 2. OCV-SOC characteristic curve.

The internal-resistance fitting and resistance distribution shown in Figures 3 and 4 establish the ohmic resistance scale used in the power-closure calculation. Figure 3 demonstrates a positive correlation between discharge current and voltage drop, validating the first-order ohmic approximation adopted in the electrical model. Although the scattered measurements contain dynamic fluctuations caused by transient operating conditions, the fitted trend line captures the dominant linear relationship required for the current-solution process. The corresponding resistance distribution in Figure 4 reveals that the estimated ohmic resistance is concentrated within a relatively narrow interval around the mean value, indicating that the identified parameter remains physically stable under the selected operating conditions. These results support the physical parameterization of the model while avoiding unnecessary expansion into a separate parameter-identification study.

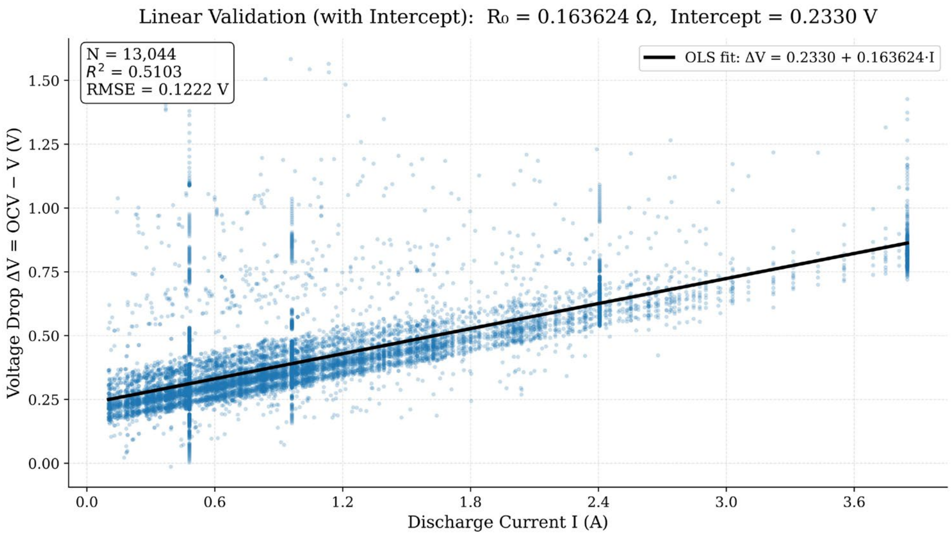

Figure 3. Internal resistance linear fitting.

ISSN 2616-5775 Vol. 9, Issue 7: 34-43, DOI: 10.25236/AJCIS.2026.090705

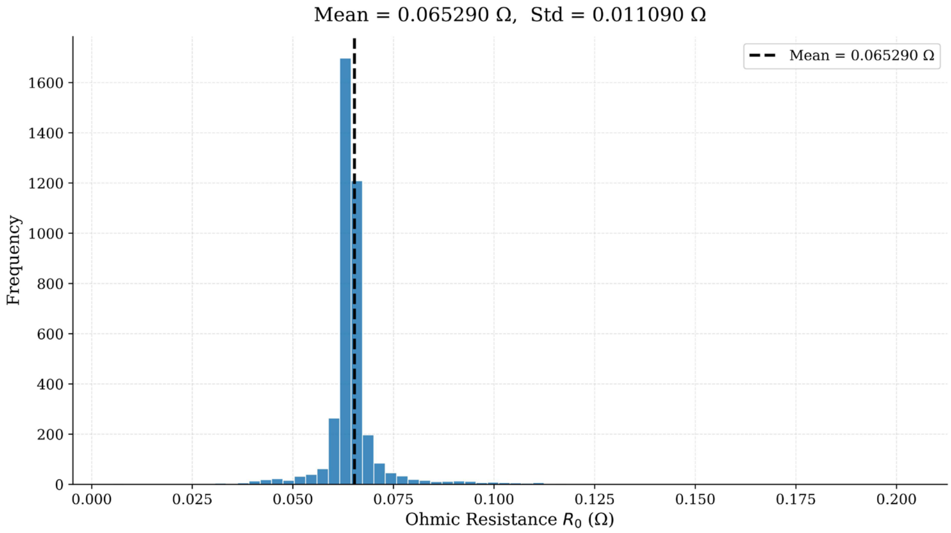

Figure 4. Internal resistance distribution.

The thermal response in Figure 5 illustrates the temperature evolution produced by the electro-thermal coupling mechanism. The predicted temperature variation closely follows the measured thermal trajectory, while the residual distribution remains bounded within a relatively small range throughout the discharge process. This agreement suggests that the lumped thermal model is capable of reproducing the dominant heat-generation and heat-dissipation behavior without introducing excessive thermal complexity. Moreover, the results confirm the existence of the electro-thermal feedback pathway: higher current produces stronger Joule heating, temperature rise modifies the effective resistance, and the altered resistance subsequently affects current and SOC depletion.

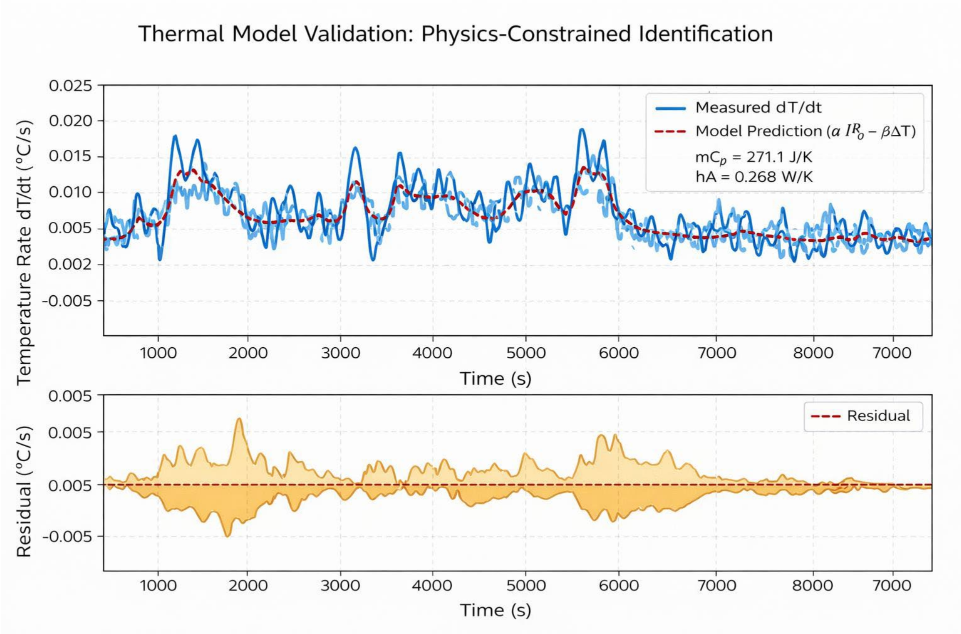

Figure 5. Electro-thermal model validation under dynamic discharge conditions

The SOC trajectory in Figure 6 demonstrates that the model generates a continuous discharge path and an explicit TTE under a representative usage profile. The SOC evolution exhibits different depletion rates under varying load intensities, reflecting the direct influence of user behavior on battery endurance. During high-load intervals, the discharge current increases significantly, leading to accelerated SOC decay and stronger voltage fluctuations, whereas lower-load stages correspond to slower energy depletion. The coupled voltage-current-SOC behavior confirms that the proposed framework can dynamically respond to realistic usage variations rather than relying on fixed discharge assumptions.

ISSN 2616-5775 Vol. 9, Issue 7: 34-43, DOI: 10.25236/AJCIS.2026.090705

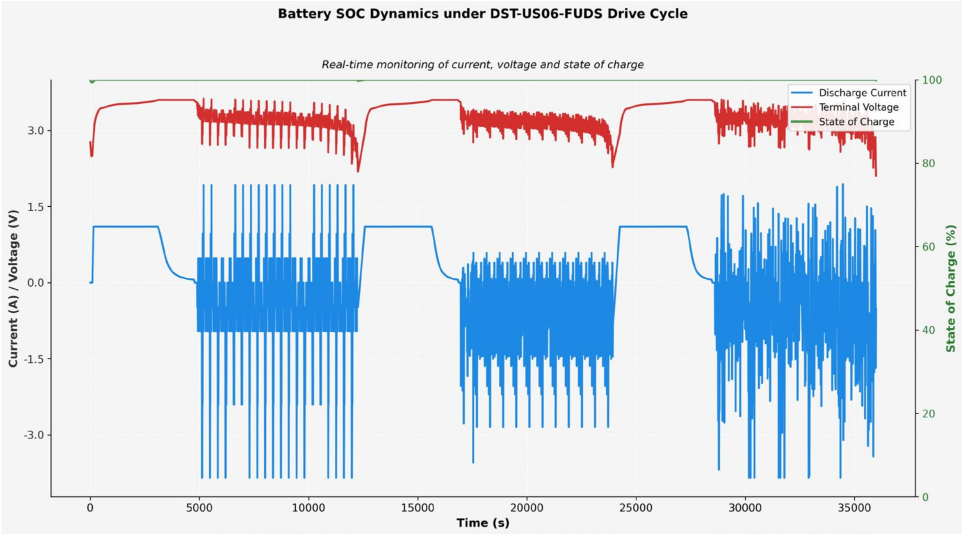

Figure 6. Dynamic evolution trajectory of SOC.

Together, these results verify the operational logic of the framework: user behavior determines power demand, power closure determines current, current drives heat generation and SOC depletion, and the depletion threshold determines TTE. The framework therefore preserves both physical interpretability and engineering applicability while remaining sufficiently compact for parameter-sensitivity analysis and practical battery-management studies.

4. Sensitivity analysis and discussion

Sensitivity analysis is used to identify the dominant sources of TTE variation. An one-at-a-time (OAT) perturbation scheme is applied to 11 parameters representing battery capacity, internal resistance, temperature coefficients, thermal properties, behavioral load weights, and environmental temperature: Q_{eff}, R_0, k_T, k_Q, k_{eta}, mC_p, hA, w_{cpu}, w_{screen}, $w_{network}$, and T_{env}. For each perturbation, the discharge process is simulated from SOC=1.0 to the depletion threshold, and TTE as well as selected SOC arrival times are recorded.

Table 1 presents the subsystem-level importance values. The results show a pronounced hierarchy. The capacity/energy scale contributes 59.30% of the sensitivity coefficient, and the load-side behavior-to-power mapping contributes 37.72%. Thermal and environmental effects contribute 2.99%, whereas electrical resistance and efficiency-temperature terms show near-zero contribution under the selected TTE metric.

Table 1. Importance of factors in OAT sensitivity analysis.

Subsystem	Importance Sensitivity Coefficient (%)	Importance Time Variation (%)
Battery Side: Capacity/Energy Scale	59.30	42.17
Load Side: Behavior-to-Power Consumption (Equivalent Load)	37.72	54.40
Thermal Side: Environment and Dissipation	2.99	3.43
Electrical Side: Internal Resistance and Temperature Dependence	0	0
Battery Side: Efficiency/Temperature Effect	0	0

This hierarchy is consistent with the charge-conservation structure of the model. When voltage varies moderately and thermal correction remains limited, the SOC decay rate is primarily governed by the relationship dSOC/dt proportional to -I/Q_eff. Consequently, TTE is directly sensitive to usable capacity and average discharge current. Capacity uncertainty changes the available charge scale, while screen, CPU, and network loads change the current through P_dem and P_act. These two mechanisms therefore dominate TTE sensitivity.

The relatively small thermal contribution should be interpreted in a metric-dependent manner. It does not imply that thermal physics is negligible. Rather, under the selected load condition and with TTE as the output metric, thermal parameters affect TTE mainly through an indirect pathway:

ISSN 2616-5775 Vol. 9, Issue 7: 34-43, DOI: 10.25236/AJCIS.2026.090705

temperature rise changes resistance, capacity correction, and efficiency, which then weakly modifies current and SOC depletion. If the target metric were peak temperature, voltage sag, thermal safety margin, or high-load degradation, the importance of thermal and resistance parameters would likely increase.

The near-zero contribution of resistance and efficiency terms should be interpreted similarly. These terms remain necessary for physical feasibility, voltage-current closure, and model consistency. Their weak first-order sensitivity indicates limited identifiability with respect to TTE under the baseline scenario and perturbation range, not physical irrelevance. This distinction is important when translating sensitivity results into engineering decisions.

5. Engineering implications

The sensitivity results suggest a clear priority order for smartphone endurance prediction and optimization. First, accurate estimation of usable capacity and SOH should be treated as a prerequisite for reliable TTE prediction. Because capacity/energy scale dominates the TTE response, an inaccurate Q_{eff} can produce substantial prediction error even when the load model is well calibrated.

Second, load-side control is the most direct pathway for extending endurance during normal operation. Reducing screen brightness, limiting sustained CPU load, scheduling background tasks, and adapting network activity under poor signal conditions all reduce P_{dem} and the average discharge current. These interventions act on the second dominant sensitivity channel and are therefore expected to provide greater TTE gains than small refinements of thermal parameters under ordinary usage.

Third, thermal optimization remains necessary as a secondary control layer. Although its first-order contribution to TTE is limited in the present setting, thermal behavior affects safety, user comfort, throttling, and high-load operation. The proposed framework can accommodate thermal-aware policies by modifying $P_{max}(S,T)$, calibrating hA, or extending the lumped thermal model to a multi-node thermal network.

Aging effects can be incorporated without changing the core structure of the model. In an aging-aware extension, fixed effective capacity and resistance are replaced by slow-varying parameters $Q(n)$ and $R(n,T)$:

$$Q_{eff}(T,n) = Q(n)\left[1 - k_Q \,|\, T - T_{ref} \,|\right], \quad R(T,n) = R(n,T) \tag{14}$$

where n denotes cycle count or battery life stage. This extension permits TTE simulation for both fresh and aged batteries within the same SOC-TTE framework. Detailed capacity-impedance fitting, impedance evolution surfaces, and lifecycle-dominant analysis are outside the main scope of this paper and can be treated as a separate degradation-focused study.

6. Conclusion

The proposed study develops a physics-grounded continuous-time electro-thermal framework for smartphone battery SOC and TTE prediction by explicitly coupling user behavior, power demand, electrical feasibility, thermal dynamics, and charge depletion. Unlike purely data-driven regression approaches, the model preserves a clear causal structure linking screen activity, CPU workload, network usage, and background processes to discharge current, temperature evolution, and SOC attenuation. Through the power-closure mechanism and electro-thermal feedback pathway, the framework maintains both physical interpretability and numerical stability under dynamically varying operating conditions.

Experimental results demonstrate that the proposed framework can realistically reproduce the nonlinear OCV-SOC relationship, current-dependent voltage drop, thermal evolution, and continuous SOC discharge trajectory observed under representative smartphone usage conditions. The fitted OCV curve and resistance distribution provide physically meaningful parameterization for the terminal-voltage and power-closure equations, while the thermal validation confirms that the lumped heat-balance model captures the dominant Joule-heating and heat-dissipation behavior without excessive model complexity. The resulting SOC trajectories further verify that the framework can dynamically respond to varying load intensities and generate explicit TTE predictions under realistic behavior-driven usage profiles.

ISSN 2616-5775 Vol. 9, Issue 7: 34-43, DOI: 10.25236/AJCIS.2026.090705

Sensitivity analysis reveals a pronounced hierarchical structure in the drivers of battery endurance. The capacity/energy scale and load-side behavior-to-power mapping dominate the TTE response, contributing 59.30% and 37.72% of the sensitivity coefficient, respectively, whereas thermal-environmental factors contribute only a secondary effect under the selected TTE metric. These findings indicate that the primary determinants of endurance are the available charge scale and the average discharge current induced by user behavior. The relatively weak first-order sensitivity of thermal and resistance parameters does not imply physical irrelevance; rather, it reflects the fact that their influence on TTE is transmitted indirectly through coupled electro-thermal pathways under the baseline operating scenario.

From an engineering perspective, the proposed framework provides a compact yet extensible foundation for smartphone battery-management studies. The results suggest that accurate SOH and usable-capacity estimation should be prioritized for reliable TTE prediction, while load-side interventions such as brightness reduction, CPU-load management, adaptive network control, and background-task scheduling provide the most direct pathway for extending endurance during normal operation. Although thermal optimization exhibits limited first-order influence on TTE in the present setting, it remains important for safety, throttling, and high-load reliability. Furthermore, the framework can naturally incorporate aging-aware extensions through slow-varying capacity and resistance functions without altering the core SOC-TTE structure. Overall, the proposed continuous-time electro-thermal framework achieves a balance between physical fidelity, engineering interpretability, and computational compactness, making it suitable for practical endurance prediction and intelligent battery-management applications.

References

[1] R. Pereira, H. Matalonga, M. Couto, F. Castor, B. Cabral, P. Carvalho, S. M. de Sousa, and J. P. Fernandes, "GreenHub: A large-scale collaborative dataset to battery consumption analysis of Android devices," Empirical Software Engineering, vol. 26, no. 3, article 38, 2021.
[2] S. Alawnah and A. Sagahyroon, "Modeling of smartphones power using neural networks," EURASIP Journal on Embedded Systems, vol. 2017, article 22, 2017.
[3] C. Yoon, S. Lee, Y. Choi, R. Ha, and H. Cha, "Accurate power modeling of modern mobile application processors," Journal of Systems Architecture, vol. 81, pp. 17-31, 2017.
[4] A. Schuler and G. Kotsis, "A systematic review on techniques and approaches to estimate mobile software energy consumption," Sustainable Computing: Informatics and Systems, article 100919, 2024.
[5] D. Bernardi, E. Pawlikowski, and J. Newman, "A general energy balance for battery systems," Journal of the Electrochemical Society, vol. 132, no. 1, pp. 5-12, 1985.
[6] X. Hu, S. Li, and H. Peng, "A comparative study of equivalent circuit models for Li-ion batteries," Journal of Power Sources, vol. 198, pp. 359-367, 2012.
[7] A. Seaman, T.-S. Dao, and J. McPhee, "A survey of mathematics-based equivalent-circuit and electrochemical battery models for hybrid and electric vehicle simulation," Journal of Power Sources, vol. 256, pp. 410-423, 2014.
[8] Z. Li, J. Huang, B. Y. Liaw, and J. Zhang, "On state-of-charge determination for lithium-ion batteries," Journal of Power Sources, vol. 348, pp. 281-301, 2017.
[9] G. L. Plett, "Extended Kalman filtering for battery management systems of LiPB-based HEV battery packs: Part 3. State and parameter estimation," Journal of Power Sources, vol. 134, no. 2, pp. 277-292, 2004.
[10] M. A. Hannan, M. S. H. Lipu, A. Hussain, and A. Mohamed, "A review of lithium-ion battery state of charge estimation and management system in electric vehicle applications: Challenges and recommendations," Renewable and Sustainable Energy Reviews, vol. 78, pp. 834-854, 2017.
[11] C. Forgez, D. V. Do, G. Friedrich, M. Morcrette, and C. Delacourt, "Thermal modeling of a cylindrical LiFePO4/graphite lithium-ion battery," Journal of Power Sources, vol. 195, no. 9, pp. 2961-2968, 2010.
[12] X. Lin, H. E. Perez, S. Mohan, J. B. Siegel, A. G. Stefanopoulou, Y. Ding, and M. P. Castanier, "A lumped-parameter electro-thermal model for cylindrical batteries," Journal of Power Sources, vol. 257, pp. 1-11, 2014.
[13] A. Barre, B. Deguilhem, S. Grolleau, M. Gerard, F. Suard, and D. Riu, "A review on lithium-ion battery ageing mechanisms and estimations for automotive applications," Journal of Power Sources, vol. 241, pp. 680-689, 2013.
[14] M. Berecibar, I. Gandiaga, I. Villarreal, N. Omar, J. Van Mierlo, and P. Van den Bossche, "Critical review of state of health estimation methods of Li-ion batteries for real applications,"

ISSN 2616-5775 Vol. 9, Issue 7: 34-43, DOI: 10.25236/AJCIS.2026.090705

Renewable and Sustainable Energy Reviews, vol. 56, pp. 572-587, 2016.
[15] P. Iurilli, C. Brivio, and V. Wood, "On the use of electrochemical impedance spectroscopy to characterize and model the aging phenomena of lithium-ion batteries: A critical review," Journal of Power Sources, vol. 505, article 229860, 2021.